International Journal of Remote Sensing
Vol. 26, No. 1, 10 January 2005, 9–27

Taylor & Francis
Taylor & Francis Group

AVHRR automated detection of volcanic clouds

A. BONFIGLIO†, M. MACCHIATO†, N. PERGOLA‡, C. PIETRAPERTOSA‡ and V. TRAMUTOLI*§

†INFM, Dipartimento di Scienze Fisiche, Università Federico II, Napoli, Monte S. Angelo, Italy

‡Istituto di Metodologie per l'Analisi Ambientale–CNR, C. da S. Loja, 85050 Tito Scalo (PZ), Italy

§Dipartimento di Ingegneria e Fisica dell'Ambiente, Università degli Studi della Basilicata, Campus Macchia Romana, 85100 Potenza, Italy; tel: +39 971 205205; fax: +39 971 205160; Email: tramutoli@unibas.it

(*Received 21 January 1998; in final form 29 June 2004*)

A new satellite-based technique has recently been proposed which seems suitable for an automatic detection of volcanic clouds in daytime conditions. In this paper the robustness of such a new approach, in particular in detecting early eruptive clouds, is evaluated, on several eruptive events at Mt Etna, by using five years of Advanced Very High Resolution Radiometer (AVHRR) data. The detection scheme is discussed together with its possible extension to night-time monitoring and the improvements expected by its application to the next generation of satellite sensors (in particular Spinning Enhanced Visible and Infrared Imager (SEVIRI)) with enhanced spectral and temporal resolution. The proposed approach seems to overcome the limitations related to other proposed methods which, in some conditions (very fresh eruptive clouds, cold-backgrounds, etc.), give false or missed detection and will no longer be applicable to the next generation of Geostationary Operational Environmental Satellites (GOES) due to the planned reduction of their thermal infrared channels until 2010.

1. Introduction

Volcanic ash clouds, injected into the atmosphere as a consequence of eruptive events, can represent a potential danger for aircraft flights (Hanstrum and Watson 1983, Casadevall 1994) by putting both passengers and crew in severe risk and causing airlines economic concern (Casadevall 1994).

Several satellite-based techniques for detecting volcanic clouds have been developed and, in some cases, used globally for this purpose. Satellites, in fact, can offer global coverage, low costs and high frequency of observation, to provide a powerful tool for an effective monitoring system.

One of the applications of satellite-based observations is the early warning of the event in progress in order to mitigate hazards and damages (Prata 1989, D'Amours 1994, Rose and Schneider 1996, Schneider *et al.* 1999).

Satellite-based techniques devoted to such a purpose find their main difficulties in discriminating volcanic clouds from water/ice clouds. In fact, all kinds of clouds are generally highly reflective in the visible part of the solar spectrum and they absorb

*Corresponding author.

International Journal of Remote Sensing
ISSN 0143-1161 print/ISSN 1366-5901 online © 2005 Taylor & Francis Ltd
http://www.tandf.co.uk/journals
DOI: 10.1080/0143116042000274122

Earth radiation in the thermal infrared. Therefore, refined methods are required in order to discriminate volcanic clouds from water/ice clouds.

To achieve this, several techniques have been proposed, which mainly rest on volcanic aerosol multispectral signatures in the infrared and visible atmospheric windows. Among the others, the Brightness Temperature Difference (BTD) method proposed by Prata (1989) exploits the reverse absorption effect in thermal infrared bands around 11 μm and 12 μm; this leads to negative values of brightness temperature differences $\Delta T = T_{11\,\mu m} - T_{12\,\mu m}$ due to the presence of liquid H_2SO_4 droplets which are often associated with volcanic clouds in the disperse phase. On the other hand, positive ΔT values are expected for water/ice clouds. Prata's approach has been widely and successfully employed, using data from geostationary (e.g. Geostationary Operational Environmental Satellite (GOES)) and polar satellite (e.g. Advanced Very High Resolution Radiometer (AVHRR)), for real-time tracking of volcanic ash clouds and, in some cases, even for thousands of kilometres and up to several days after the main eruption (e.g. Schneider *et al.* 1995, Davies and Rose 1998, Rose *et al.* 2001). The main advantage of this approach is its applicability during both day and night and its simplicity that makes it easy to use with little operator intervention. The main limitations are:

(a) its declared (e.g. Wen and Rose 1994, Rose *et al.* 1995, Schneider *et al.* 1995, Krotkov *et al.* 1999) inability to detect very fresh eruptive clouds which, in the first few minutes, might contain water droplets and/or ice particles and, then, are very difficult to be distinguished from meteorological clouds in the infrared (IR) data;
(b) its doubtful reliability when the temperature contrast between the ash cloud and the underlying surface is not large enough (Wen and Rose 1994, Rose and Schneider 1996, Seftor *et al.* 1997); and
(c) its loss of performance (Simpson *et al.* 2000) in the presence of high atmospheric water vapour content (e.g. maritime and tropical climate regions).

Furthermore, some of the above-quoted authors (e.g. Wen and Rose 1994, Rose *et al.* 1995) realize that the above-mentioned reverse effect (i.e. negative value of ΔT) completely disappears for particles greater than 5 μm. Although such an approach is routinely applied by several Volcanic Ash Advisory Centres (VAACs) by using both GOES and National Oceanic and Atmospheric Administration (NOAA)/AVHRR imagery, its actual reliability has recently been hotly questioned (Simpson *et al.* 2000, 2001, Prata *et al.* 2001). Even if other methods, based on satellite thermal infrared sounding, exist (e.g. Ellrod and Connell 1999), the need for new satellite '… techniques for automatic detection of volcanic eruptions with as low a false alarm rate as possible (optimally $<5\%$) …' persists, since 1999, as a high priority in the annual reports of the Volcanic Hazards Team of the Committee on Earth Observation Satellites, Disaster Management Support Group (CEOS-DMSG). In order to make up for the loss of GOES 12 μm channel (from 2002 to 2010), the CEOS-DMSG Final Report (CEOS 2001) continues to include a recommendation to '… develop alternative sources … or additional multi-spectral techniques …' for volcanic eruptions and ash cloud monitoring.

Other methods exist (e.g. Holasek and Self 1995) which exploit spectral signatures of volcanic clouds in the visible/near-infrared bands. Although water/ice clouds and atmospheric aerosol layers increase the albedo in visible and near-infrared spectral regions (Lyons and Husar 1976), this does not happen in the visible in the same way

as in the infrared region. It has been found (Rao *et al.* 1989), for instance, that for aerosols the effect is much more marked in the visible AVHRR channel 1 (0.58–0.68 μm) than in the near-infrared AVHRR channel 2 (0.725–1.1 μm), so that the ratio of reflectances measured in channels 1 and 2 (ch1/ch2) could also be used in order to discriminate volcanic clouds from water/ice clouds. As shown by Rao *et al.* (1989) and confirmed by model computations (Masuda *et al.* 1988) expected values for this ratio, observed over sea locations, should be greater than 1.3 for aerosol clouds and very close to, or slightly less than, 1 when meteorological clouds are present. In spite of a very good sensitivity in cases of weak gas or ash emissions as well as when early eruption clouds are considered, the main drawbacks of such a method are, of course, its restriction to daytime observations over sea locations and a decreasing reliability observed in the case of denser volcanic clouds. The technique proposed by Rao *et al.* (1988), which makes use of AVHRR infrared channels 3 (3.55–3.93 μm), 4 (10.5–11.3 μm) and 5 (11.5–12.5 μm), in addition to cloud screening criteria based on visible and near-infrared reflectance, in order to distinguish atmospheric aerosols from clouds, seems to be similarly sensitive to local observation conditions.

A different technique was proposed by Pergola *et al.* (1998, 2001) which, on the basis of visible/near-infrared NOAA/AVHRR data, seems to permit an automatic and reliable volcanic cloud detection during daytime. It is based on the general Robust AVHRR Techniques (RAT) approach proposed by Tramutoli (1998) and already successfully applied to several other natural emergencies, like forest fires (Cuomo *et al.* 2001) and earthquakes (Tramutoli *et al.* 2001a).

In this paper the robustness of such a new approach, in particular in detecting early eruptive clouds, is evaluated on several eruptive events at Mt Etna; its possible extension to night-time monitoring is discussed together with the improvements expected by its application to the next generation of satellite sensors (in particular to Spinning Enhanced Visible and Infrared Imager (SEVIRI), on the Meteosat Second Generation platform) with increased spectral and temporal resolution.

2. The general RAT approach

The RAT approach is an automatic change-detection scheme that considers a satellite image as a realization of a space–time process, described at each place (x, y) and time t, by the value of the satellite derived measurement $V(x, y, t)$. It identifies signal anomalies in the space–time domain as deviations from a normal state that has been preliminarily identified on the basis of satellite observations collected during several years, in similar observational conditions, for each image pixel and period of the year. In order to identify anomalous signal transients the Absolutely Local Index of Change of Environment (ALICE) is computed as follows:

$$\otimes_V(x, y, t) \equiv \frac{V(x, y, t) - V_{REF}(x, y)}{\sigma_V(x, y)} \tag{1}$$

where $V_{REF}(x, y)$ is a reference field (the time average, the minimum or the maximum, depending on the specific application) which describes the expected value of the signal $V(x, y, t)$ in unperturbed conditions and $\sigma_V(x, y)$ is the standard deviation, being both computed on historical records collected in observational conditions as similar as possible (same time of the day, same month of the year, etc.) to the ones of the image to be processed. The ALICE gives then, for each image pixel (x, y) and time t of observation, the *llocal* deviation of the signal $V(x, y, t)$

(weighted by its historically observed *llocal* variability) from its expected value $V_{REF}(x, y)$ in unperturbed conditions. This (double l) was first introduced by Tramutoli (1998) and it emphasizes the dependence on the place and time of observation.

The robustness of this approach is intrinsic, because higher signal variability $\sigma_V(x, y)$ (in the chosen spatial/temporal domain) will result in lower values of $\otimes_V(x, y, t)$ reducing, in this way, the problem of false alarm proliferation often associated to the traditional *fixed threshold* approaches. The RAT approach has already been applied to the study of volcanic (Pergola *et al.* 2001, Tramutoli *et al.* 2001b) and meteorological (Tramutoli *et al.* 2000) clouds, to forest fires (Cuomo *et al.* 2001) and earthquakes (Tramutoli *et al.* 2001a). Its application to the detection of volcanic eruptive clouds on the basis of AVHRR observations in the visible spectral range will be described in §4.

3. Data used

NOAA/AVHRR data collected at the Istituto di Metodologie per l'Analisi Ambientale (IMAA) High Resolution Picture Transmission (HRPT) receiving station in Tito (15° 40′ E, 40° 35′ N) were calibrated in reflectances, for channels 1 (0.58–0.68 μm) and 2 (0.725–1.05 μm), and in brightness temperatures, for channels 4 (10.3–11.3 μm) and 5 (11.5–12.5 μm) following standard calibration procedures described by Lauritson *et al.* (1979) and by Rao and Chen (1996).

Special attention was given to geo-referencing procedures in order to obtain the best image-to-image co-location and to reduce errors due to navigation inaccuracy. Hence a precise navigation was performed following the automatic method proposed by Pergola and Tramutoli (2000). An extended dataset of AVHRR imagery, collected between 1994 and 2001, was then precisely navigated, co-registered and re-mapped to the same Lambert Azimuthal Area projection with a residual error estimated to be within one AVHRR pixel (1.1 km at nadir view).

Several Etna eruption events were considered for validation, chosen in different seasonal periods and associated with eruptive plumes of different intensities. Table 1 gives the details of NOAA satellite passes corresponding to the eruptive events described in this paper. Pass A was received during a period of a documented intense strombolian activity of the Bocca Nuova crater which started abruptly on 24 December 1990 keeping up a strong, continuous ash emission, until the beginning of January 1991 (Anon 1991). Pass C, on 23 December 1995, was recorded just at the beginning of an intense Etna eruption which developed its plume up to a maximum

Table 1. Data used: NOAA satellite identification and date of pass are indicated for AVHRR imagery related to the events discussed in the paper.

Pass	Date	Event description	Satellite and time of acquisition
A	12 January 1991	Strombolian activity	NOAA-11 12:51 GMT
B	21 December 1995	Not documented	NOAA-14 12:33 GMT
C	23 December 1995	Eruptive activity	NOAA-14 12:11 GMT
D	19 July 2001	Eruptive activity	NOAA-16 11:40 GMT
Reference dataset	January, December and July in between 1994 and 1998	No documented activity	235 NOAA-14 and NOAA-16 passes around 12:00 GMT

height of 10 km. This is a major documented eruptive event which occurred after a quiescent period of about two years (M. Coltelli, personal communication 1996, Privitera *et al.* 1996a). Pass D refers to the latest strong flank eruption which occurred on 17–18 July 2001, characterized by new fissures opening around the Montagnola site at 2100 and 2700 m elevation. In particular, the new vent, which opened at 2700 m elevation, on the evening of 18 July, became explosive producing very strong strombolian explosions and towering ash columns (Behncke 2001). There was a relatively high risk for the town of Nicolosi and the lava flow represented a serious threat to the cable car station and Rifugio Sapienza.

Figure 1 shows the visible channel of AVHRR passes corresponding to the three events described. In reference to the case of December 1995 (pass C), taking into account the time delay due to the acquisition rate of AVHRR (6 lines/s) and the relative position of Mt Etna on the scene, the volcano area appears as observed from the satellite at approximately 12:16 GMT, that is about 16 min after the paroxysm in the recorded volcanic tremor amplitude (Privitera *et al.* 1996b) and a few seconds after the observed beginning (at 12:15 GMT, M. Coltelli, personal communication 1996) of the eruptive phase.

Pass B in table 1 refers to a minor event (on 21 December 1995, two days before the 23 December eruption) considered in order to test the sensitivity of the proposed technique also to weak and/or pre-eruptive volcanic emissions.

The wind fields analyses elaborated by the European Centre for Medium-range Weather Forecast (ECMWF) for different levels of pressure and at 0.5° of resolution (both in latitude and longitude), were also analysed in order to give an account of observed volcanic plume shapes and dynamics.

It should be noted that all the selected satellite passes (except pass B) refer to the early stages of eruption phases. This is not a fortuitous choice inasmuch as it is particularly under such conditions that traditional detection schemes fail (Simpson *et al.* 2000, 2001) and, on the other hand, early detection of the volcanic cloud represents a real need for aircraft safety (Salinas 1999).

4. Detection of volcanic clouds

In order to discriminate meteorological from volcanic clouds, the BTD method proposed by Prata (1989) was initially checked. Some results, related to three of the above-mentioned Etna eruptive events, are shown in figure 2. It is easy to recognize that the simple BTD test fails in detecting volcanic clouds (figure 2(*c*)), sometimes (figures 2(*a*) and 2(*b*)) erroneously classifying meteorological clouds as volcanic ones. This is probably due to the fact that we are dealing with the early stage of the eruptions. Very likely, in the case of the winter events depicted in figures 2(*a*) and 2(*b*), the presence of a cold background has further reduced the sensitivity of such a technique (Wen and Rose 1994). In all cases volcanic plumes appear associated with relatively lower, but positive, ΔT values that prevent the BTD *fixed threshold* test from correctly identifying the plume. This result seems to confirm a strong dependence of the effectiveness of BTD discrimination criterion ($\Delta T<0$) on the observation conditions and on ash cloud properties.

In order to overcome such problems a different approach, based on the use of *llocal thresholds* automatically provided by the application of the general RAT approach (see §2), has been applied in this work. Following Pergola *et al.* (2001) it has been implemented by the following steps:

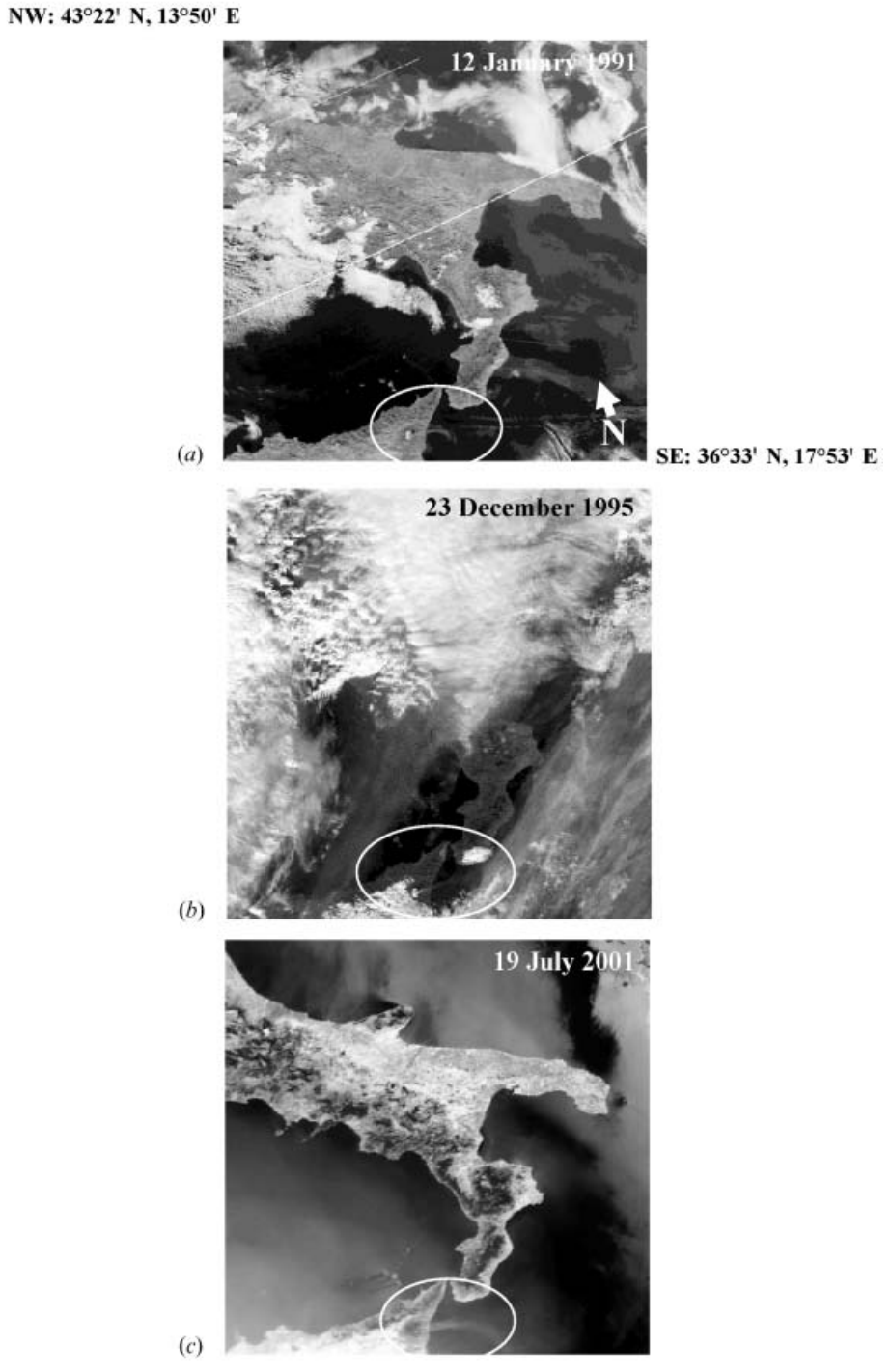

Figure 1. AVHRR visible reflectance fields (channel-1) for NOAA passes described in table 1: (*a*) pass A, 12 January 1991; (*b*) pass C, 23 December 1995; and (*c*) pass D, 19 July 2001. The data analysed are 512×512 sized sub-scenes in the same (Lambert azimuthal) projection. Brighter shades of grey correspond to higher values of reflectance. White circles indicate Mt Etna eruptive plumes.

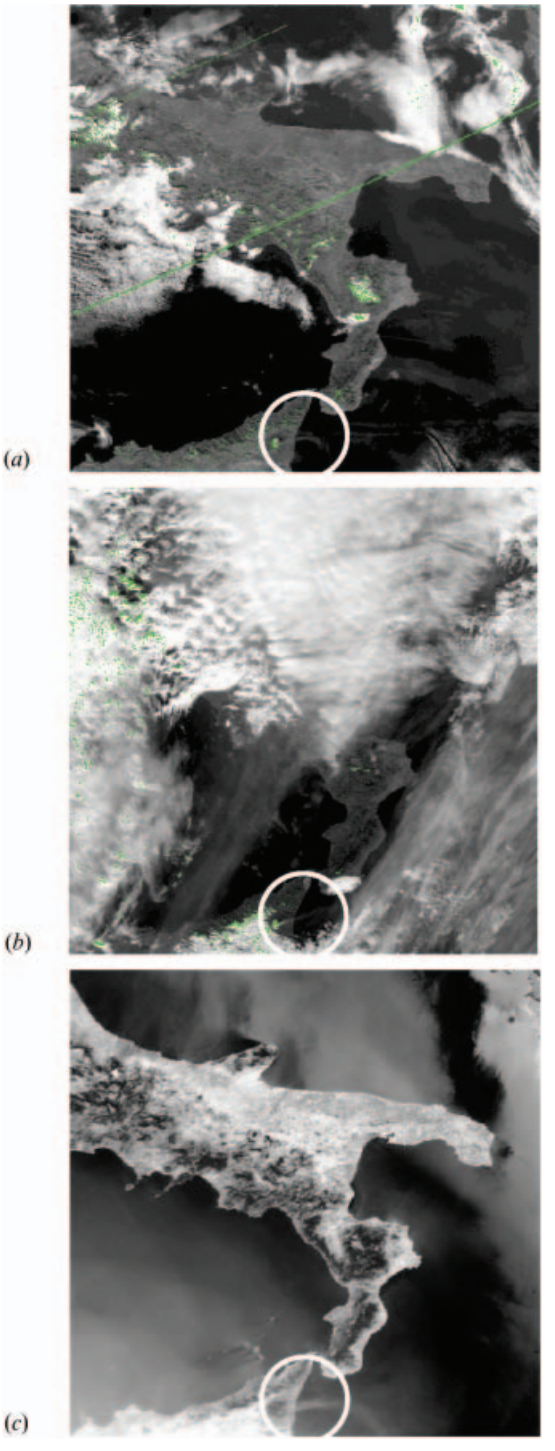

Figure 2. BTD test findings: as in figure 1 with pixels associated to negative values of $\Delta T = T_{11\,\mu m} - T_{12\,\mu m}$ depicted in green, respectively for pass A (*a*), pass C (*b*) and pass D (*c*). Note that volcanic plume is never detected. Moreover several erroneous identifications are produced by the BTD test both in (*a*) and (*b*) cases.

(a) Detection of meteorological clouds.
(b) Computation of visible reflectance reference fields.
(c) Detection of volcanic clouds.

4.1 *Detection of meteorological clouds*

In order to identify meteorological clouds the ch1/ch2 ratio test (Rao *et al.* 1989) was applied. Results obtained for the same satellite passes (A, C and D) depicted in figures 1 and 2, are shown in figure 3. Looking at the green pixels, flagged by the test as 'cloudy', (i.e. with a ch1/ch2 ratio less than 1.3 over sea locations), it is safe to argue that such a discrimination test was successful in recognizing meteorological clouds in all the events analysed. Meteorological clouds, in fact, were properly recognized so that remaining pixels (including the ones related to the volcanic cloud) can be rightly retained for further processing.

Consequently, for all the AVHRR imagery used throughout this work, the ch1/ch2 ratio test was applied first in order to identify pixels affected by meteorological clouds and to exclude them from the subsequent analysis.

4.2 *Construction of a reference field for reflectances in the visible AVHRR channel 1*

In order to define a *normal* reference field (i.e. in absence of anomalous particle loading related to volcanic activity) for visible reflectances in AVHRR channel 1, a statistical analysis was performed over the sequence of AVHRR scenes selected on the basis of criteria of homogeneity of observation conditions, according, in particular, to the season and to the hour of satellite pass (Tramutoli 1998, Pergola *et al.* 2001). Only satellite passes of the same period and time were considered in order to avoid spurious effects due to the relative Sun, and satellite positions. Obviously, all cloudy pixels were rejected by means of the above-mentioned ch1/ch2 screening test.

A minimum value composite (mVC) procedure (Pergola *et al.* 2001) was applied to the imagery so that, for each location (x, y), the minimum value $\rho_{MIN}(x, y)$ of visible reflectance $\rho(x, y, t)$ in AVHRR channel 1 was retained. This procedure, which was applied only over sea locations previously identified as cloud-free, is expected to minimize the effects of

(a) residual contamination from clouds and/or aerosols which have higher reflecting properties (in the visible band) than the sea background; and
(b) image-to-image differences in Sun–satellite relative position (off-nadir view being generally associated to higher visible reflectances).

Such a procedure gives, for each location, a reference minimum reflectance value which, by construction, is associated with conditions of maximum atmospheric transparency.

At this stage some other aspects should be considered in order to make such a method fully reliable, they are

(a) the possible presence of spurious reflectance minima due to phenomena, such as cloud shadows or oil slicks (Böhm *et al.* 1991, Legg 1991, Stephens and Matson 1993), generally not related to an actual increase of atmospheric transparency; and
(b) the possible selection of reflectance minima associated with fluctuations in atmospheric aerosols which are natural or, in any case, not related to volcanic activity. This is the case, for example, of marine aerosols, whose

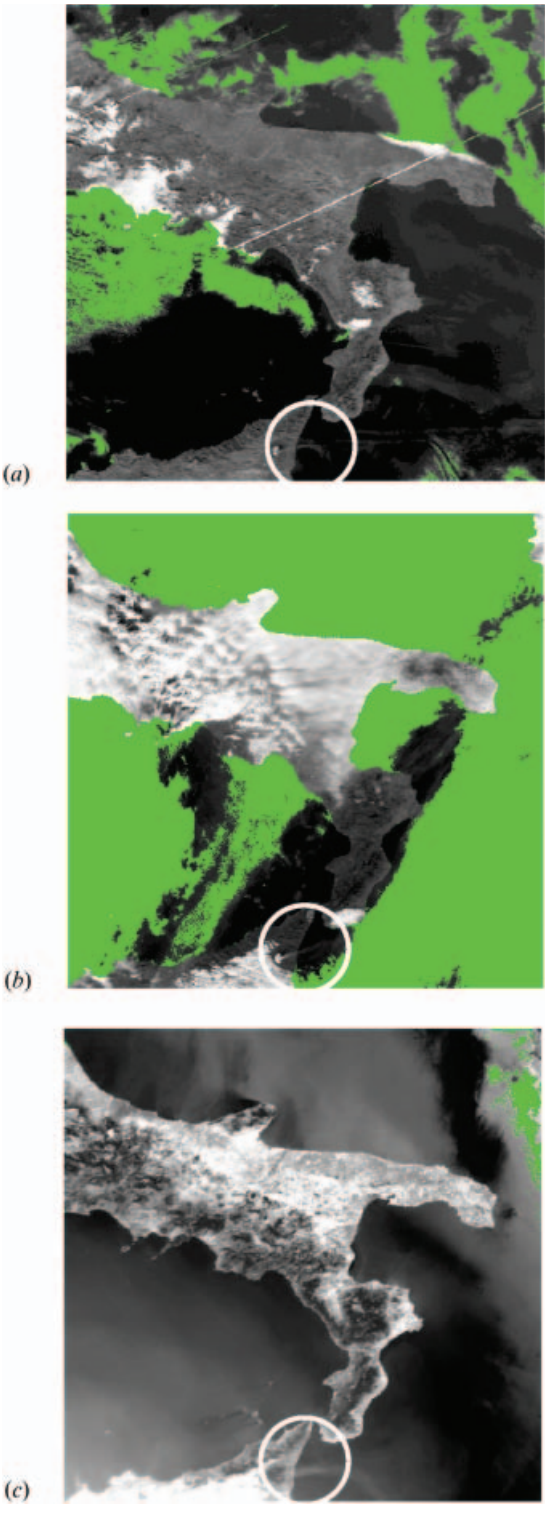

Figure 3. Ch1/Ch2 ratio test results: as in figure 1 with cloudy pixels, over the sea, coloured in green, respectively for pass A (*a*), pass C (*b*) and pass D (*c*).

natural production is highly variable, especially near the coast, depending on wind direction and intensity (Despiau *et al.* 1996).

The following consideration can be deduced:

- A preliminary screening of the imagery is required in order to eliminate spurious reflectance minima.
- Local time-variability of the reflectance field must also be considered in order to distinguish between anomalies in the visible reflectance field related to volcanic aerosols and the normal variability due to other (i.e. non-volcanic) sources.

Both of these requirements were taken into account by carrying out a 3σ-clipping automatic filter, excluding from further processing all pixels having $|\rho(x, y, t) - \langle\rho(x, y)\rangle| > 3\sigma_\rho(x, y)$ where $\langle\rho(x, y)\rangle$ is the calculated mean reflectance and $\sigma_\rho(x, y)$ is the respective standard deviation. Afterwards, a new computation of local composite minimum $\rho'_{\min}(x, y) = mVC(x, y)$, mean $\langle\rho'(x, y)\rangle$ and standard deviation $\sigma'_\rho(x, y)$ is performed by using only pixels which survived from the preceding step. The process is iterated until no more data have to be excluded.

This procedure (described in detail by Tramutoli 1998) is mainly devoted to obtaining two fields, minimum reflectance $\rho'_{\min}(x, y)$ and standard deviation $\sigma'_\rho(x, y)$, which are expected to represent, for each location, visible reflectance and its observed variability, in normal conditions (i.e. in absence of aerosol burden related to volcanic activity).

Figure 4 gives an example of how the described procedure works, being able to recognize automatically a spurious reflectance minimum associated with a cloud shadow. It refers to the computation of $\rho_{\min}(x, y)$ and $\sigma_\rho(x, y)$ reference fields for the month of December and for the time around 12:00 GMT, performed on the basis of five years of co-located AVHRR imagery collected (in December and around 12:00 GMT) in between 1994 and 1998.

Figures 4(*a*) and 4(*c*) represent the $\rho_{\min}(x, y)$ and $\rho'_{\min}(x, y)$ fields as obtained respectively before and after 3σ-clipping filter application. Major differences appear in a long trail of low reflectance values (dark on the false colour picture) which, extending from west to east opposite to the Sicilian coast, disappears moving from figure 4(*a*) to figure 4(*c*). Looking at figure 4(*b*), where the visible AVHRR channel is shown for one of NOAA-14 passes used for the reference field generation (orbit 10103 at 12.42.22 GMT on 15 December 1996), it is easy to recognize that we were in the presence of a single-image effect, related to a well marked cloud shadow that the algorithm was able to detect and eliminate automatically.

It should be noted that the 3σ-clipping filter acts at a pixel level so that, for example, only part of the previously examined scene was rejected. This circumstance is especially important when having to work with a relatively poor sample of measurements.

Figure 5 shows the obtained $\sigma'_\rho(x, y)$ reference field for the same time (around 12:00 GMT) and period of the year (December). High values of $\sigma'_\rho(x, y)$ (in brighter shades of grey) are generally localized in the proximity of coasts according with the expected, above-mentioned, effect due to marine aerosols production and variability.

4.3 *Detection of volcanic clouds*

In the previous paragraphs we summarized the technique used in order to generate the $\rho'_{\min}(x, y)$ and $\sigma'_\rho(x, y)$ reference fields for a specific area, by means of a series of

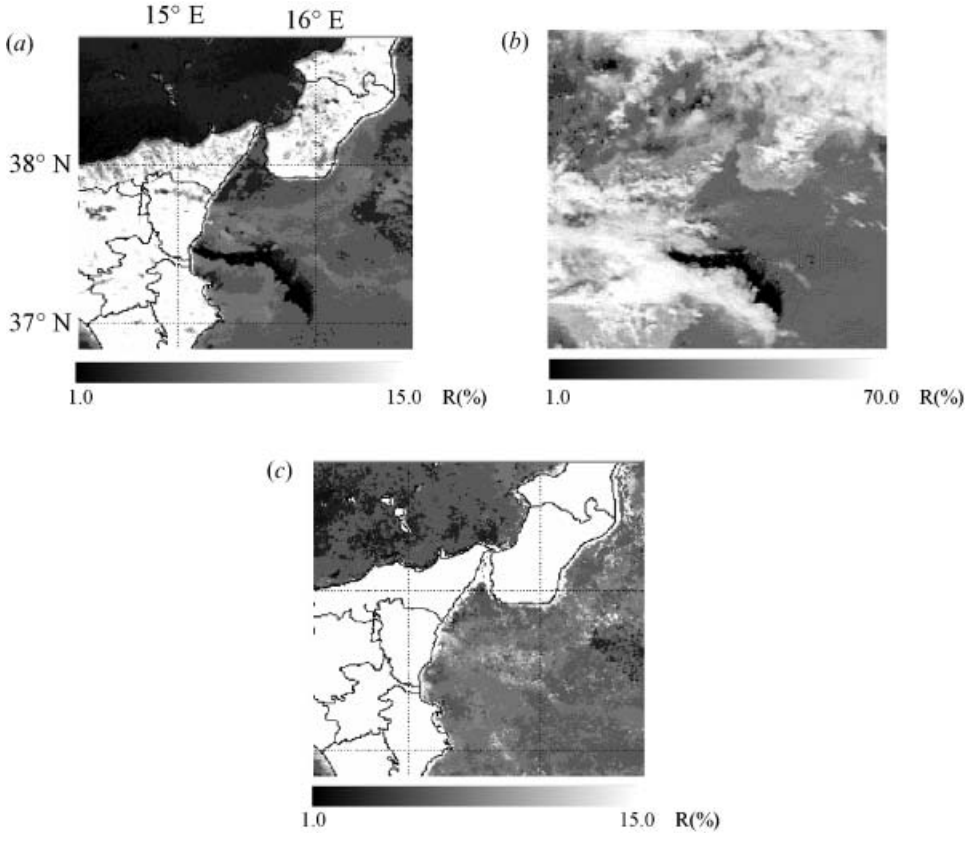

Figure 4. Elimination of spurious reflectance minima by $3\sigma_\rho$-clipping filter: (*a*) the $\rho_{\min}(x, y)$ minimum composite reference field computed considering the whole dataset of co-located AVHRR imagery (channel 1) collected in December around 12:00 GMT between 1994 and 1998; (*b*) AVHRR channel 1 for NOAA-14, orbit 10103 on 15 December 1996: note the long cloud shadow in the centre of the image responsible for the spurious reflectance minima similarly present in the initial $\rho_{\min}(x, y)$ reference field; and (*c*) the $\rho'_{\min}(x, y)$ reference field after the application of the filter. Note that the above-mentioned spurious reflectance minima have been removed.

AVHRR scenes collected in unperturbed periods (i.e. far enough from documented volcanic events) and similar seasonal and observational conditions (Sun and satellite's zenithal angles, time of pass, etc.).

By using AVHRR data coming from the IMAA historical archive (which includes images from 1980 until now), $\rho'_{\min}(x, y)$ and $\sigma'_\rho(x, y)$ fields were produced for the months of January, July and December in order to evaluate the performances of the proposed technique in the case of the events which occurred at Mt Etna during the months of January 1991, December 1995 and July 2001. A total number of 235 AVHRR sub-scenes, of 512×512 pixels, were analysed in order to produce the above-defined background reference fields.

According to expression (1) a Statistically Normalized Albedo Excess (SNAE) index was then computed (Pergola *et al.* 1998, 2001) for each AVHRR image at hand as:

$$SNAE(x, y, t) = \frac{\rho(x, y, t) - \rho'_{\min}(x, y)}{\sigma'_\rho(x, y)} \tag{2}$$

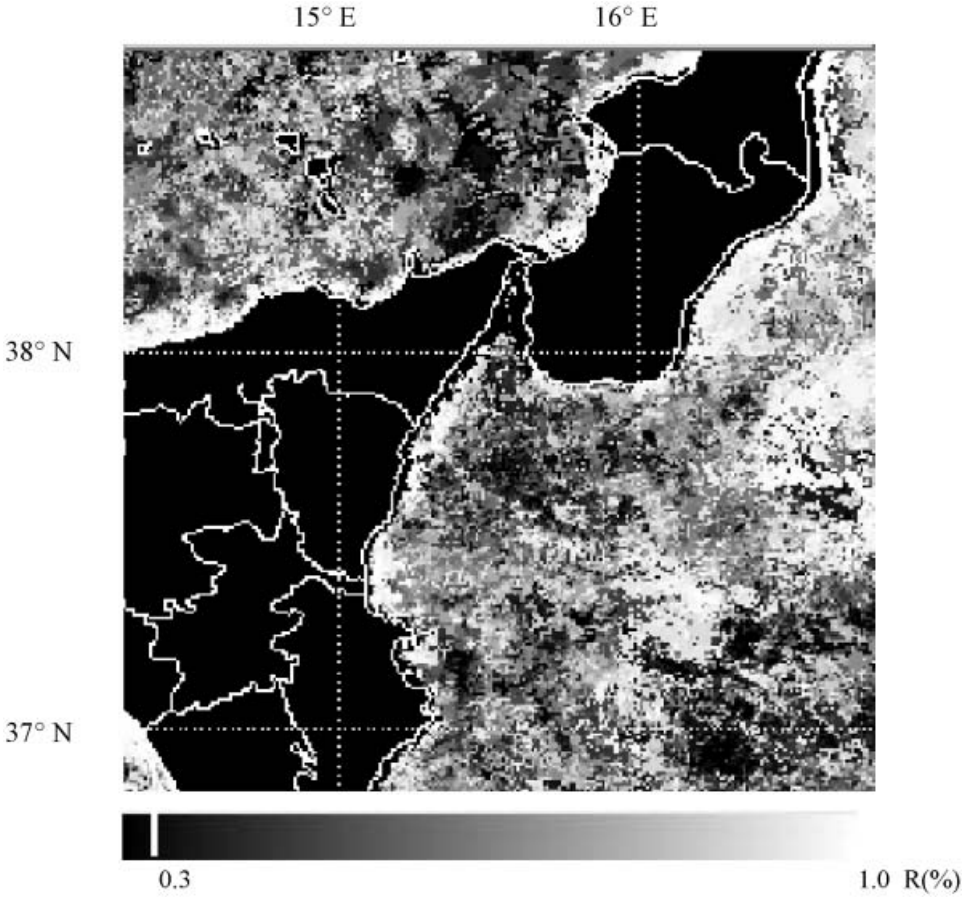

Figure 5. The $\sigma'_\rho(x, y)$ reference field for AVHRR channel 1 (dataset: December around 12:00 GMT, years 1994–1998, see text): zoom on the study area. Brighter shades of grey correspond to higher values of $\sigma'_\rho(x, y)$. Land locations are masked in black colour.

where $\rho(x, y, t)$ is the visible reflectance value (AVHRR channel-1) measured at location (x, y) at time t. In expression (2) the numerator gives the local albedo excess compared to the $\rho'_{\min}(x, y)$ reference value of the signal; the denominator $\sigma'_\rho(x, y)$ gives the amount of the *normal* (i.e. in unperturbed conditions) variability of the signal at the same place. In this way, the SNAE index gives an indication of the amount of the albedo excess weighted by the *normal* variability of the signal historically observed at the same location (x, y) in similar seasonal and observational conditions.

5. Results

Results of the above-described analysis are shown in figure 6 (to be compared with BTD results in figure 2) and in figure 7.

On the right-hand side of figure 6, *SNAE* values are depicted in false colours for passes A, C and D. Only values greater than 1 (i.e. albedo excess greater than its *normal* local variability σ'_ρ) over sea locations are shown. On the left-hand side the same portion of the scene, as observed in AVHRR channel 1, is represented. It is evident that higher values of *SNAE* indicate very well the presence of a volcanic

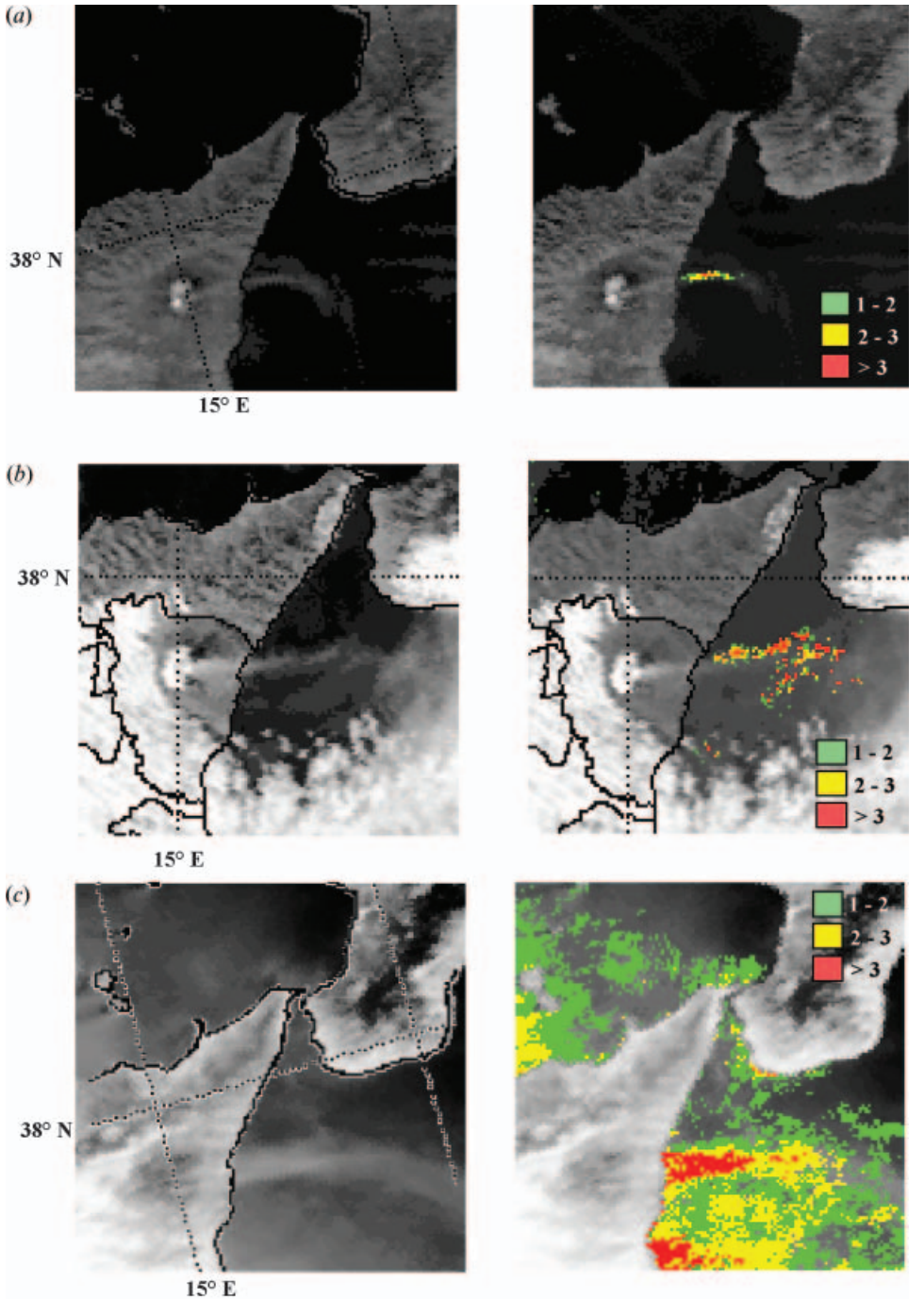

Figure 6. *SNAE* analysis results (zooms on the study area as in figure 5). On the right side pixels with *SNAE*(x, y, t) values greater than 1 (only over the sea) are represented in different colours for (from top to bottom) passes A (*a*), C (*b*) and D (*c*). On the left side the same portion of the scene, as observed in AVHRR channel 1, is represented. Note that highest *SNAE* values, on the investigated region, are unequivocally associated to volcanic plumes (see text).

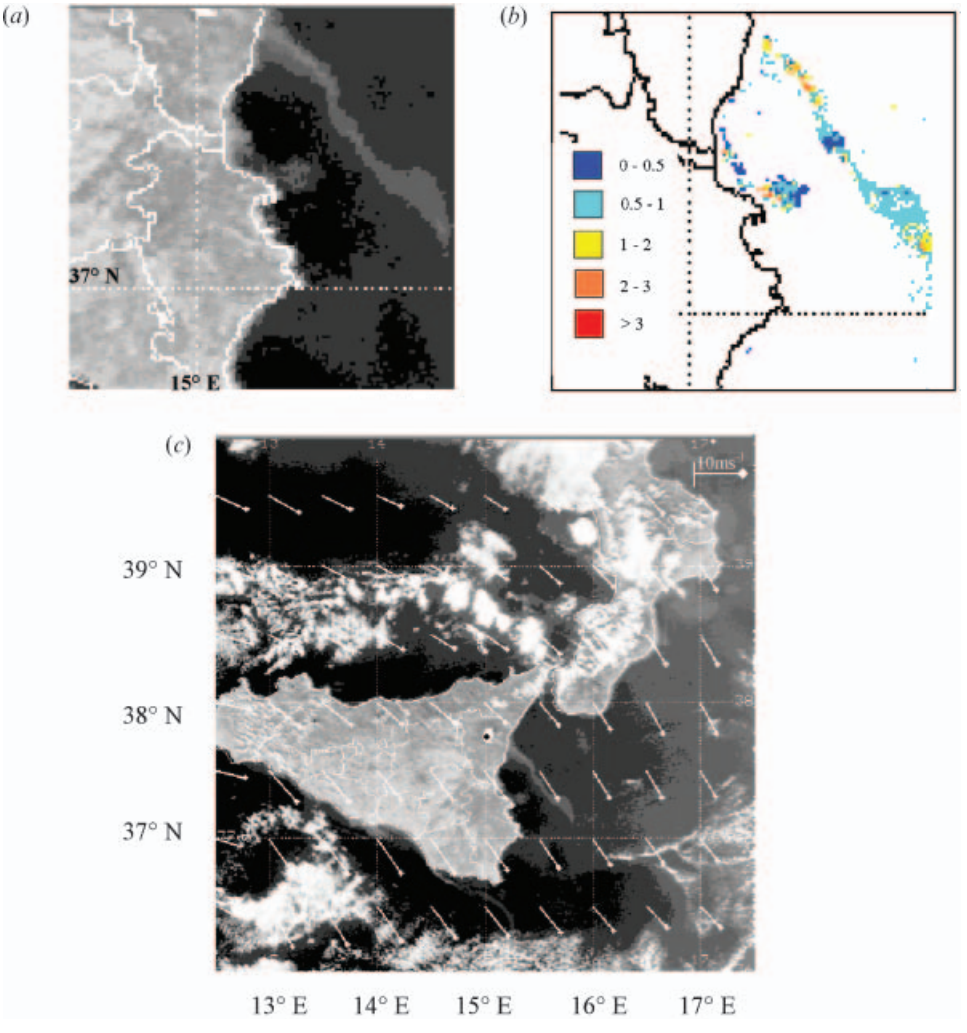

Figure 7. Detection of very weak volcanic emissions, 21 December 1995: (*a*) AVHRR channel 1 for pass B; (*b*) values of *SNAE* computed for the same day; and (*c*) ECMWF wind field analysis for 850 mbar pressure level and 12:00 GMT (enlarged view): wind intensity and direction are indicated by white arrows.

plume without confusing it with meteorological clouds also in the case of (as in figure 6(*b*)) nearby clouds. Looking at the *SNAE* products it is possible to note that the volcanic plume is always detected even if, in figure 6(*a*) for the event of January 1991, the observed anomaly is not so intense (*SNAE* values never greater than 3). On the other hand, although the image in figure 6(*c*) related to the eruption of July 2001 is partly affected by the sun-glint effect (note the bright areas over the sea in figure 1(*c*)) which produces a more 'noisy' *SNAE* field, the eruptive plume is all the same unequivocally identified by the highest *SNAE* values.

With regard to the event of 23 December 1995, the same test was performed on available satellite passes for days preceding the eruption. The first useful (not completely overcast) satellite pass found was the one (pass B in table 1) of 21 December. Results of the test are presented in figure 7. Also in this case, the higher

SNAE values (figure 7(*b*)) seem to provide a correct identification of an aerosol emission unequivocally associable with the Mt Etna activity. This is confirmed by the simple inspection of figure 7(*a*) and further corroborated by the wind field analysis (at 850 mb and 12:00 GMT) of ECMWF shown in figure 7(*c*). Looking at these figures it is quite evident, without the necessity of back-trajectory computations, that the spatial evolution of the plume, starting from Mt Etna, follows the dominant wind direction at the plume height. The identification of this emission as a possible preparatory event of the following eruption, is not in the ambitions of this paper. Nevertheless, this possibility is not to be excluded looking also at records of Mt Etna Permanent Seismic Network which show an increased volcanic tremor amplitude starting at 18:00 local time on 22 December (Privitera *et al.* 1996b).

A minor effect (with some *SNAE* values higher than 2), is also evident, both in figures 7(*a*) and 7(*b*), along the coast. Its direct correlation with Mt Etna activity is not equally evident. It is, however, suggested from the apparent bifurcation of the *SNAE* field probably due to local meteorological conditions.

The 21 December event is, to our knowledge, not otherwise documented (in particular not by ground-based observations).

The presence of detectable volcanic emissions preceding eruptive phases could be regarded as a possible precursor signal for impending eruptions (Malinconico 1979) but, as stated before, this aspect is not a target of this work. What we would like to stress here is that the proposed technique seems able automatically to detect and recognize also very weak (e.g. not eruptive) volcanic emissions (as already demonstrated in the case of Pinatubo's stratospheric clouds, Tramutoli *et al.* 2001b) which are not always detected, as in the circumstance discussed above, by traditional volcano monitoring networks.

Finally it should be emphasized that such definite results would not be achievable by using only the $\rho'_{\min}(x, y)$ field. It is, in fact, the weighting function, $\sigma'_{\rho}(x, y)$, which permits us to evaluate visible reflectance excesses not only with respect to the most favourable atmospheric (high transparency) and observational (close to nadir) conditions, but also with regards to their *llocal* normal variability, avoiding false alarms due to anomalous signals not related to the phenomenon under consideration (Tramutoli 1998). In conclusion, the *SNAE* index seems *robust* enough to avoid false identifications (as the ones described in figures 2(*a*) and 2(*b*)) but sensitive enough to identify correctly the presence of volcanic plumes of different thickness in different observation conditions.

6. Final remarks

The technique proposed in this paper seems to overcome the limitations related to the use of the BTD method, which fails in some conditions (pre-eruptive clouds, cold-backgrounds, etc.) and will no longer be applicable to the next generation of GOES satellites due to the planned reduction of their thermal infrared channels.

It strongly rests on the knowledge of *normal* behaviour and variability of the investigated signal, which can be achieved from the analysis of homogeneous historical satellite records. As it is based only on satellite data at hand, it can easily be reproduced for different geographical areas and seasons and exported to different satellite packages. In particular it might be immediately exported to the next generation of satellite sensors with improved capabilities in terms of repetition rate, spectral and spatial resolution, providing a powerful tool for operational purposes.

Among the others should be mentioned SEVIRI (on the Meteosat Second Generation platform): it offers an image every 15 min and a selection of channels which saves and strongly extends the present AVHRR capability for volcanic activity monitoring from space.

Several aspects must be considered which strongly suggest that better results are to be expected from the extension of the proposed method to this satellite package.

(a) The improved quality of the image-to-image superposition together with the preservation of the same angle of view for each portion of the scene (offered by the geostationary attitude) will reduce the observational noise due to navigation and co-location errors as well as to the changes of view angles (and consequently of ground resolution cells).
(b) The improved temporal resolution will reduce both the natural (lower image-to-image variability of the signal at each location) and observational (greater homogeneity of time-series elements) noise.

Both effect (a) and (b) will produce a reduction of the term $\sigma'_\rho(x, y)$ in expression (2), consequently increasing the sensitivity of *SNAE* toward relatively lower signal variations even in the presence of a reduced (compared with AVHRR) spatial resolution.

In this paper a qualitative approach, devoted only to an automatic detection of volcanic aerosols, has been voluntarily chosen, but this does not exclude possible quantitative developments. In fact, as a relatively low reduction (less than 1.7%) of AVHRR channel 1 radiance can be expected as a consequence of an ozone amount increasing up to about 25% and, thanks to the observed linear correlation between $\rho(x, y, t)$ and atmospheric turbidity (Masuda *et al.* 1988) over low albedo surfaces, the local visible reflectance excess $\Delta\rho = \rho(x, y, t) - \rho'_{\min}(x, y)$ could represent itself (by its definition) a measure of the atmospheric turbidity even if, for some applications, it could require an absolute calibration. These applications, nevertheless, will surely benefit by the information content on local surface optical properties, stored inside the $\rho'_{\min}(x, y)$ reference field. The lack of knowledge of visible surface reflectance, so highly variable (spatially and temporally) over land, represents in fact one of the main weaknesses of traditional methods (Kaufman and Sendra 1988, Masuda *et al.* 1988, Rao *et al.* 1988, 1989, Wen and Rose 1994) devoted to giving a quantitative estimate of several atmospheric aerosol properties.

For the same reason, we expect improvements from an extended use of the *SNAE* index in order to identify inter-annual trends or short-term anomalies, in atmospheric turbidity, particularly in areas where the tropospheric aerosol background is high (e.g. air-polluted industrial or metropolitan areas) and, therefore, daily environmental monitoring is much more necessary (Pergola *et al.* 1998).

Finally we would like to emphasize that the proposed approach could also be extended toward the traditional detection techniques that, as observed in this work and in other studies (Simpson *et al.* 2000), produce results which are critically dependent on the values of some assumed thresholds. Following the same approach, for example, suitable BTD thresholds, might be automatically established for each place and observational time on the basis of properly chosen (homogeneous) historical satellite records.

In any case, as in most observational conditions (more aged, semi-transparent volcanic clouds, minor presence of water/ice droplets in ash clouds, smaller particle

sizes, etc.) the BTD test has demonstrated its effectiveness, a possible complementary use of both techniques (in daytime) could be suggested in order to overcome the problems related to particular observational conditions.

All these possibilities, together with the extension to other observation conditions (i.e. over land locations), represent the natural continuation of this work.

Acknowledgments

This work was supported by ASI (Agenzia Spaziale Italiana) within the framework of FASA Project (contract number I/R/203/02) and funded by the European Community and Regione Basilicata in the context of POP-FESR 1994–1996—'Timoran'—Project.

References

ANON, 1991, *Bulletin of the Global Volcanism Network*, 16:03 on web page: http://www.volcano.si.edu/gvp/volcano/region01/italy/etna/var_06.htm.

BEHNCKE, B., 2001, Italy's volcanoes, 'the Cradle of Volcanology', web page: http://www.geo.mtu.edu/~boris/ETNA_news.html.

BÖHM, E., MARULLO, S. and SANTOLERI, R., 1991, AVHRR visible–IR detection of diurnal warming events in the western Mediterranean Sea. *International Journal of Remote Sensing*, **12**, pp. 695–701.

CASADEVALL, T.J. (ed.), 1994, Volcanic ash and aviation safety: proceedings of the first international symposium on volcanic ash and aviation. *US Geological Survey Bulletin 2047*, p. 450.

CEOS (Committee on Earth Observation Satellites), 2001, The use of Earth Observing Satellites for hazard support: assessment and scenarios. Final report of the Disaster Management Support Group, available at the CEOS web site http://disaster.ceos.org.

CUOMO, V., LASAPONARA, R. and TRAMUTOLI, V., 2001, Evaluation of a new satellite-based method for forest fire detection. *International Journal of Remote Sensing*, **22**, pp. 1799–1826.

D'AMOURS, R., 1994, Current and future capabilities in forecasting trajectories, transport, dispersion of volcanic ash clouds at the Canadian Meteorological Centre. In *Volcanic Ash and Aviation Safety: Proceedings of the First International Symposium on Volcanic Ash and Aviation*, T.J. Casadevall (Ed.). *US Geological Survey Bulletin 2047*, p. 325.

DAVIES, M.A. and ROSE, W.I., 1998, GOES imagery fills gaps in Montserrat volcanic cloud observations. *EOS Transactions*, **79**, pp. 505–507.

DESPIAU, S., COUGNENC, S. and RESCH, F., 1996, Concentrations and size distributions of aerosol particle in coastal zone. *Journal of Aerosol Science*, **27**, pp. 403–415.

ELLROD, G.P. and CONNELL, B., 1999, Improvements in volcanic ash detection using GOES multi-spectral image data. *Proceedings of 8th Conference on Aviation, Range, and Aerospace Meteorology, Dallas, Texas, 10–15 January 1999* (Boston: American Meteorological Society), pp. 326–329.

HANSTRUM, B.N. and WATSON, A.S., 1983, A case study of two eruptions of Mount Galunggung and an investigation of volcanic eruption cloud characteristics using remote sensing techniques. *Australian Meteorological Magazine*, **31**, pp. 171–177.

HOLASEK, R.E. and SELF, S., 1995, GOES weather satellite observations and measurements of the May 18, 1980, Mount St. Helens eruption. *Journal of Geophysical Research*, **100**, pp. 8469–8487.

KAUFMAN, Y.J. and SENDRA, C., 1988, Satellite mapping of aerosol loading over vegetated areas. In *Aerosols and Climate*, P.V. Hobbs and M.P. McCormick (Eds) (Hampton, VA: A. Deepak Publishing), pp. 51–67.

KROTKOV, N.A., TORRES, O., SEFTOR, C., KRUEGER, A.J., KONSTINSKI, A., ROSE, W.I., BLUTH, G.J.S., SCHNEIDER, D. and SCHAEFER, S.J., 1999, Comparison of TOMS and

AVHRR volcanic ash retrievals from the August 1992 eruption of Mt. Spurr. *Geophysical Research Letters*, **26**, pp. 455–458.

LAURITSON, L., NELSON, G.J. and PORTO, F.W., 1979, Data extraction and calibration of TIROS-N/NOAA radiometers. NOAA Technical Memorandum NESS 107, US Department of Commerce, Washington, DC, USA.

LEGG, C.A., 1991, The Arabian Gulf oil slick, January and February 1991. *International Journal of Remote Sensing*, **12**, pp. 1795–1796.

LYONS, W.A. and HUSAR, R.B., 1976, SMS/GOES visible images detect a synoptic-scale air pollution episode. *Monthly Weather Review*, **103**, pp. 1623–1626.

MALINCONICO, L.L., 1979, Fluctuations in SO_2 emission during recent eruptions of Etna. *Nature*, **278**, pp. 43–45.

MASUDA, K., TAKASHIMA, T. and RAO, C.R.N., 1988, Remote sensing of atmospheric aerosols over the oceans using multispectral radiances measured with the Advanced Very High Resolution Radiometer onboard the NOAA meteorological satellites. In *Aerosols and Climate*, P.V. Hobbs and M.P. McCormick (Eds) (Hampton, VA: A. Deepak Publishing), pp. 38–49.

PERGOLA, N. and TRAMUTOLI, V., 2000, SANA: Sub-pixel Automatic Navigation of AVHRR imagery. *International Journal of Remote Sensing*, **21**, pp. 2519–2524.

PERGOLA, N., PIETRAPERTOSA, C. and TRAMUTOLI, V., 1998, Satellite remote sensing of volcanic aerosols: a new, AVHRR-based, approach. In *Satellite Remote Sensing of Clouds and the Atmosphere III*, J.E. Russel (Ed.). *Proceedings of SPIE,* **3495**, pp. 188–197.

PERGOLA, N., PIETRAPERTOSA, C., LACAVA, T. and TRAMUTOLI, V., 2001, Robust satellite techniques for monitoring volcanic eruptions. *Annali di Geofisica*, **44**, pp. 167–177.

PRATA, A.J., 1989, Observations of volcanic ash clouds in the 10–12 μm window using AVHRR/2 data. *International Journal of Remote Sensing*, **10**, pp. 751–761.

PRATA, A.J., BLUTH, G.J.S., ROSE, W.I., SCHNEIDER, D.J. and TUPPER, A., 2001, Comments on 'Failures in detecting volcanic ash from a satellite-based technique'. *Remote Sensing of Environment*, **78**, pp. 341–346.

PRIVITERA, E., SPAMPINATO, S., TORRISI, O. and D'AMICO, G.D., 1996a, Recent relevant episodes in volcanic tremor at Mt. Etna. Web site of Istituto Internazionale di Vulcanologia. Web page http://sismsrv.iiv.ct.cnr.it/tremetna.htm.

PRIVITERA, E., SPAMPINATO, S., TORRISI, O. and D'AMICO, G.D., 1996b, Recent relevant episodes in volcanic tremor at Mt. Etna. Web site of Istituto Internazionale di Vulcanologia. Web page http://sismsrv.iiv.ct.cnr.it/95122223/2223dice.htm.

RAO, C.R.N. and CHEN, J., 1996, Post-launch calibration of the visible and near-infrared channels of the Advanced Very High Resolution Radiometer on the NOAA-14 spacecraft. *International Journal of Remote Sensing*, **17**, pp. 2743–2747.

RAO, C.R.N., STOWE, L.L., MCCLAIN, E.P. and SAPPER, J., 1988, Development and application of aerosol remote sensing with AVHRR data from the NOAA satellites. In *Aerosols and Climate*, P.V. Hobbs and M.P. McCormick (Eds) (Hampton, VA: A. Deepak Publishing), pp. 69–79.

RAO, C.R.N., STOWE, L.L., MCCLAIN, E.P. and SAPPER, J., 1989, Remote sensing of aerosols over the oceans using AVHRR data. Theory, practice and applications. *International Journal of Remote Sensing*, **10**, pp. 743–749.

ROSE, W.I. and SCHNEIDER, D.J., 1996, Satellite images offer aircraft protection from volcanic ash clouds. *EOS Transactions*, **77**, pp. 529–530.

ROSE, W.I., DELENE, D.J., SCHNEIDER, D.J., BLUTH, G.J.S., KRUEGER, A.J., SPROD, I., MCKEE, C., DAVIES, H.L. and ERNST, G.G.J., 1995, Ice in the 1994 Rabaul eruption cloud: implications for volcano hazard and atmospheric effects. *Nature*, **375**, pp. 477–479.

ROSE, W.I., BLUTH, G.J.S., SCHNEIDER, D.J., ERNST, G.G., RILEY, C.M., HENDERSON, L.J. and MCGIMSEY, R.G., 2001, Observations of volcanic clouds in their first few days of

atmospheric residence: the 1992 eruptions of Crater Peak, Mount Spurr volcano, Alaska. *Journal of Geology*, **109**, pp. 677–694.

SALINAS, L., 1999, Volcanic ash clouds pose a real threat to aircraft safety. *Proceedings of the 8th Conference on Aviation, Range, and Aerospace Meteorology, Dallas, Texas, 10–15 January 1999* (Boston: American Meteorological Society), pp. 322–325.

SCHNEIDER, D.J., ROSE, W.I. and KELLEY, L., 1995, Tracking of 1992 eruption clouds from Crater Peak Vent of Mount Spurr Volcano, alaska, using AVHRR. *US Geological Survey Bulletin*, **2139**, pp. 27–36.

SCHNEIDER, D.J., ROSE, W.I., COKE, L.R., BLUTH, G.J.S., SPROD, I.E. and KRUEGER, A.J., 1999, Early evolution of a stratospheric volcanic eruption cloud as observed with TOMS and AVHRR. *Journal of Geophysical Research*, **104**, pp. 4037–4050.

SEFTOR, C.J., HSU, N.C., HERMAN, J.R., BHARTIA, P.K., TORRES, O., ROSE, W.I., SCHNEIDER, D.J. and KROTKOV, N., 1997, Detection of volcanic ash clouds from Nimbus-7/TOMS reflectivity data. *Journal of Geophysical Research*, **102**, pp. 16749–16759.

SIMPSON, J.J., HUFFORD, G.L., PIERI, D. and BERG, J.S., 2000, Failures in detecting volcanic ash from a satellite-based technique. *Remote Sensing of Environment*, **72**, pp. 191–217.

SIMPSON, J.J., HUFFORD, G.L., PIERI, D. and BERG, J.S., 2001, Response to 'Comments on "Failures in detecting volcanic ash from a satellite-based technique"'. *Remote Sensing of Environment*, **78**, pp. 347–357.

STEPHENS, G. and MATSON, M., 1993, Monitoring the Persian Gulf war with NOAA AVHRR data. *International journal of Remote Sensing*, **14**, pp. 1423–1429.

TRAMUTOLI, V., 1998, Robust AVHRR techniques (RAT) for environmental monitoring: theory and applications. In *Earth Surface Remote Sensing II*, G. Cecchi and E. Zilioli (Eds). *SPIE*, **3496**, pp. 101–113.

TRAMUTOLI, V., LANORTE, V., PERGOLA, N., PIETRAPERTOSA, C., RICCIARDELLI, E. and ROMANO, F., 2000, Self-adaptive algorithms for environmental monitoring by SEVIRI and GERB: a preliminary study. *Proceedings of the 2000 EUMETSAT Meteorological Satellite Data Users' Conference, Bologna, 29 May–2 June 2000* (Darmstadt: EUMETSAT), pp. 79–87.

TRAMUTOLI, V., DI BELLO, G., PERGOLA, N. and PISCITELLI, S., 2001a, Robust satellite techniques for remote sensing of seismically active areas. *Annals of Geophysics*, **44**, pp. 295–312.

TRAMUTOLI, V., PERGOLA, N. and PIETRAPERTOSA, C., 2001b, Training on NOAA-AVHRR of robust satellite techniques for next generation of weather satellites: an application to the study of space–ime evolution of Pinatubo's stratospheric volcanic cloud over Europe. In *IRS 2000: Current Problems in Atmospheric Radiation*, W.L. Smith and Yu. M. Timofeyev (Eds) (Hampton, VA: Deepak Publishing), pp. 36–39.

WEN, S. and ROSE, W.I., 1994, Retrieval of sizes and total masses of particles in volcanic clouds using AVHRR bands 4 and 5. *Journal of Geophysical Research*, **99**, pp. 5421–5431.